Molecular Cell, Volume *69*

Supplemental Information

Mitochondrial MDM2 Regulates Respiratory Complex I Activity Independently of p53

Giuseppe Arena, Madi Yann Cissé, Samuel Pyrdziak, Laurent Chatre, Romain Riscal, Maryse Fuentes, Jamie Jon Arnold, Markus Kastner, Laurie Gayte, Christelle Bertrand-Gaday, Kevin Nay, Claire Angebault-Prouteau, Kerren Murray, Beatrice Chabi, Christelle Koechlin-Ramonatxo, Béatrice Orsetti, Charles Vincent, François Casas, Jean-Christophe Marine, Sandrine Etienne-Manneville, Florence Bernex, Anne Lombès, Craig Eugene Cameron, Hervé Dubouchaud, Miria Ricchetti, Laetitia Karine Linares, and Laurent Le Cam

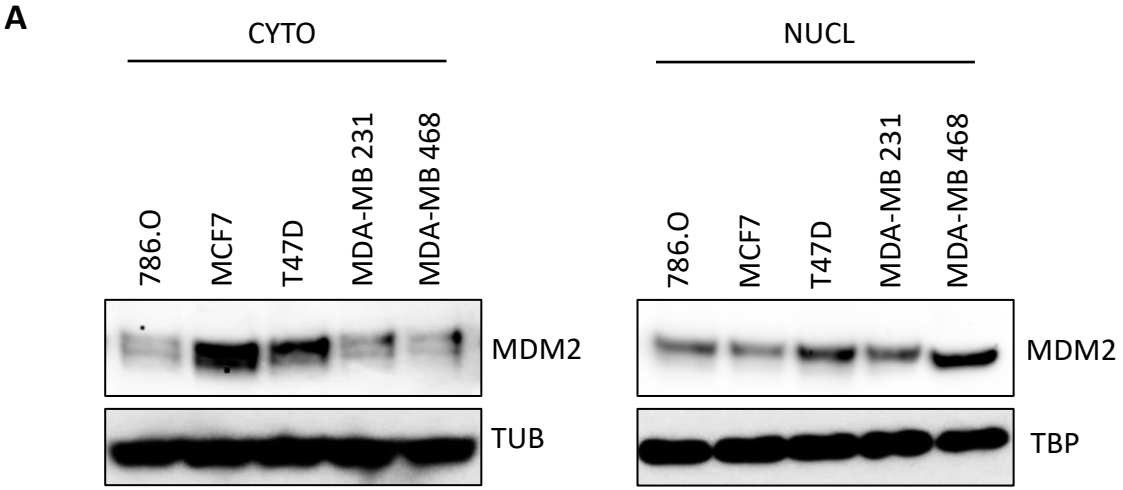
A
CYTO
NUCL
786.O
MCF7
T47D
MDA-MB 231
MDA-MB 468
MDM2
TUB
TBP

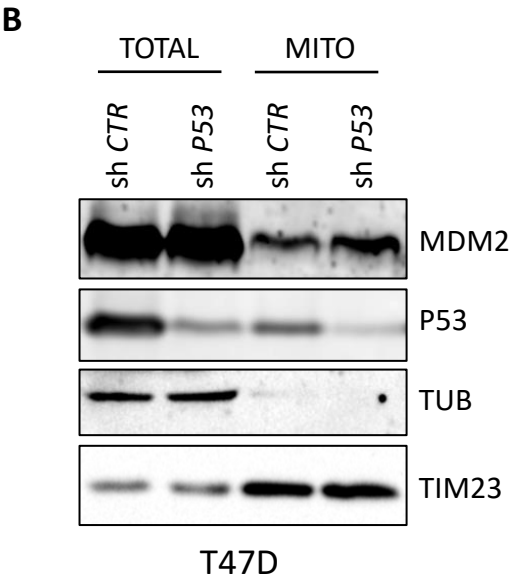
B
TOTAL
MITO
sh CTR
sh P53
MDM2
P53
TUB
TIM23
T47D

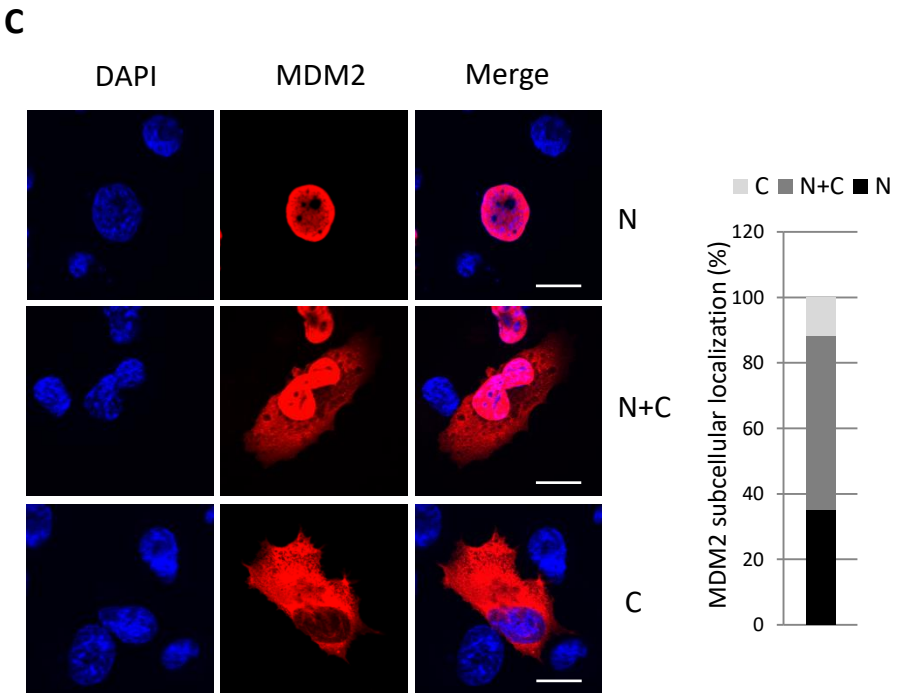
C
DAPI
MDM2
Merge
N
N+C
C
C N+C N
MDM2 subcellular localization (%)
120
100
80
60
40
20
0

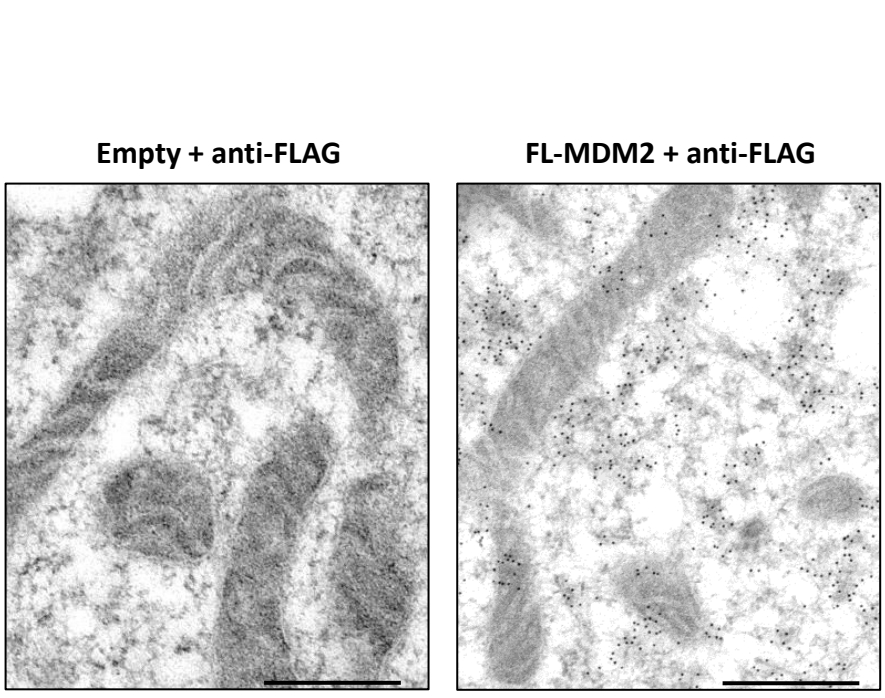
D
Empty + anti-FLAG
FL-MDM2 + anti-FLAG

Figure S1, related to Figure 1. **(A)** Immunoblot (IB) analysis of cytosolic (left panels) and nuclear (right panels) endogenous MDM2 protein levels in different human cancer cell lines. (**B**) IB analysis of endogenous MDM2 subcellular localization in T47D breast cancer cells transduced with lentiviruses encoding control or *p53* shRNAs. (**C**) Immunofluorescence (IF) analysis of MDM2 subcellular localization in H1299 cells expressing Flag-tagged full length (aa 1-491) MDM2 (FL-MDM2). MDM2 was stained with an anti-FLAG antibody (red) and nuclei were stained with DAPI (blue). Scale bar: 10 μm. Right panel: the histobar represents the percentage of cells showing different MDM2 subcellular localization (N = nuclear only; N+C = nuclear and cytoplasmic; C = cytoplasmic only; n=100 from 3 independent experiments). **(D)** Immunogold staining for electron transmission microscopy analysis of MDM2 localization in H1299 cells expressing FL-MDM2 or control cells transfected with the corresponding empty vector (Empty). Immunolabelling was performed using a monoclonal anti-FLAG antibody followed by secondary antibody conjugated to 10 nm gold particles. Specificity of the staining was confirmed by the absence of gold particles in cells transfected with the empty vector. Scale bar: 500 nM.

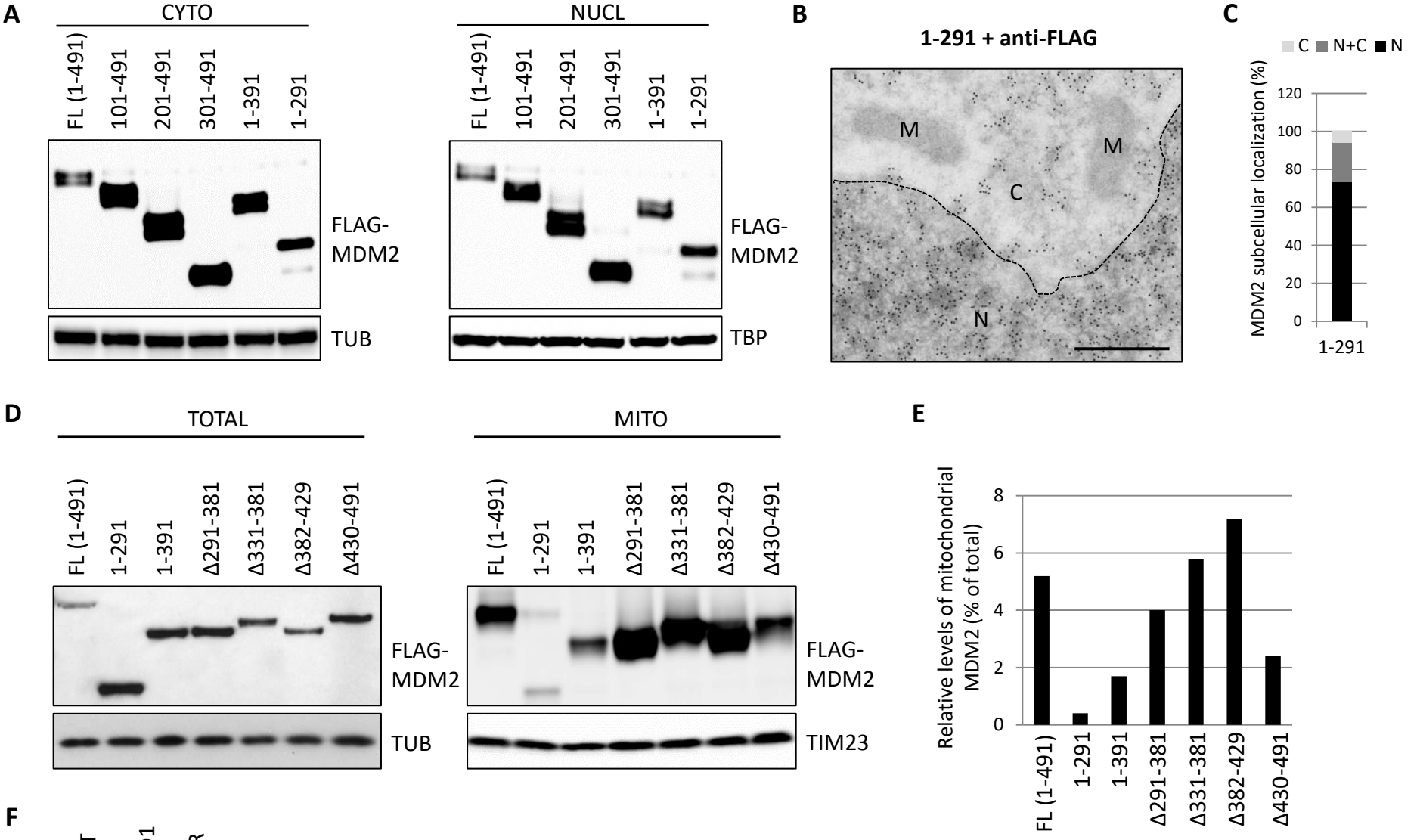
A
CYTO
NUCL
FL (1-491)
101-491
201-491
301-491
1-391
1-291
FLAG-MDM2
TUB
TBP
B
1-291 + anti-FLAG
M
C
N
C
MDM2 subcellular localization (%)
C
N+C
N
120
100
80
60
40
20
0
1-291
D
TOTAL
MITO
FL (1-491)
1-291
1-391
Δ291-381
Δ331-381
Δ382-429
Δ430-491
FLAG-MDM2
TUB
TIM23
E
Relative levels of mitochondrial MDM2 (% of total)
8
6
4
2
0
F
INPUT
IP TID1
IP CTR
MDM2
TID1

Figure S2, related to Figure 2. (**A**) The subcellular localization of FL-MDM2 and of the indicated deletion mutants was determined in fractions enriched in cytosolic (CYTO) or nuclear (NUCL) proteins prepared from transiently transfected H1299 cells. Immunoblot (IB) analysis of MDM2 protein levels was performed using anti-FLAG antibody. Equal loading was verified with TATA-BINDING-PROTEIN (TBP) and TUBULIN (TUB) protein levels. (**B**) Immunogold staining for transmission electron microscopy analysis of MDM2 localization in H1299 cells expressing a C-terminal deletion mutant of MDM2 (aa 1-291) that fails to localize in mitochondria. Scale bar: 500 nM. (**C**) Histobar represents the subcellular localization of MDM2 1-291 in H1299 cells subjected to IF analysis (N = nuclear only; N+C = nuclear and cytoplasmic; C = cytoplasmic only; n=100 from 3 independent experiments). (**D**) The subcellular localization of FL-MDM2 and of the indicated deletion mutants in H1299 cells was determined in whole-cell lysates (TOTAL) and in extracts prepared from purified mitochondria (MITO). (**E**) Histobars represent the relative amount of mitochondrial FL-MDM2 and of the indicated deletion mutants in transiently transfected H1299 cells (calculated as the % of total MDM2). (**F**) Co-immunoprecipitation assays showing association between FL-MDM2 and endogenous TID1 proteins in H1299 cells.

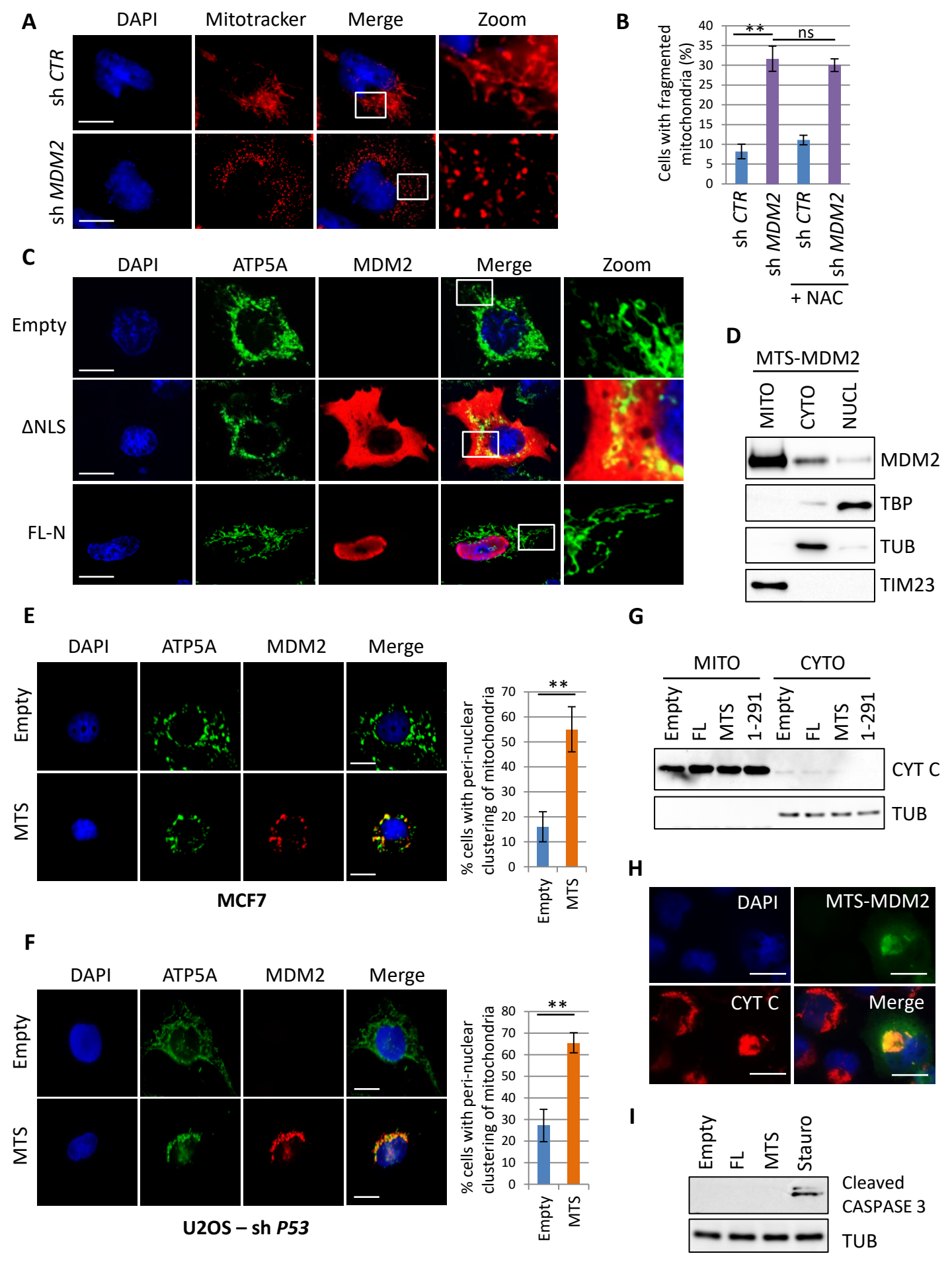
A
DAPI
Mitotracker
Merge
Zoom
sh CTR
sh MDM2
B
Cells with fragmented mitochondria (%)
**
ns
sh CTR
sh MDM2
sh CTR
sh MDM2
+ NAC
C
DAPI
ATP5A
MDM2
Merge
Zoom
Empty
ΔNLS
FL-N
D
MTS-MDM2
MITO
CYTO
NUCL
MDM2
TBP
TUB
TIM23
E
DAPI
ATP5A
MDM2
Merge
Empty
MTS
MCF7
% cells with peri-nuclear clustering of mitochondria
**
Empty
MTS
F
DAPI
ATP5A
MDM2
Merge
Empty
MTS
U2OS – sh P53
% cells with peri-nuclear clustering of mitochondria
**
Empty
MTS
G
MITO
CYTO
Empty
FL
MTS
1-291
Empty
FL
MTS
1-291
CYT C
TUB
H
DAPI
MTS-MDM2
CYT C
Merge
I
Empty
FL
MTS
Stauro
Cleaved CASPASE 3
TUB

Figure S3, related to Figure 3. (**A**) Microphotographs of H1299 cells transduced with lentiviruses encoding control- (sh *Ctr*) or *MDM2*- (sh *MDM2*) shRNAs. Mitochondria were stained with Mitotracker Red (Red) and nuclei with DAPI (blue), and then analyzed by confocal microscopy. Insets show microphotographs at higher magnification (Zoom). Scale bar, 10 µM. (**B**) Mitochondrial fragmentation in MDM2-depleted H1299 cells cultured in presence of the ROS scavenger N-Acetyl-Cysteine (NAC). Histobars represent the frequency (mean ± SEM) of cells exhibiting fragmented mitochondria (mean ± SEM; n=100 cells from 3 independent experiments). (**C**) Confocal microscopy analysis of the mitochondrial network in control (Empty) H1299 cells or in cells expressing a MDM2 mutant lacking its nuclear localization signal (ΔNLS) which expression is restricted to the cytoplasm. A representative cell expressing FL-MDM2 (FL-N) in the nucleus only is also shown (bottom panels). Mitochondria and MDM2 were detected with anti-ATP5A (green) and anti-Flag (red) antibodies, respectively. Nuclei were stained with DAPI (blue). Insets show microphotographs at higher magnification of the merged images (Zoom). Scale bar: 10 µm. (**D**) Subcellular localization of MTS-MDM2 in H1299 cells. Fractions enriched in cytosolic (CYTO), nuclear (NUCL) or mitochondrial (MITO) proteins were analyzed by immunoblotting using anti-MDM2, TBP, TUB, and TIM23 antibodies. (**E-F**) Confocal microscopy analysis of the mitochondrial network in (**E**) MCF7 cells, or (**F**) in p53-depleted U2OS cells, expressing ectopic MTS-MDM2 (MTS) or in the corresponding control cells transfected with an empty vector (Empty). ATP5A (green), MDM2 (red) and nuclei (blue). Scale bar, 10 µM. Right panels: histobars represent the frequency of cells (% of transfected) exhibiting perinuclear clustering of mitochondria (mean ± SEM; n=120 cells from 3 independent experiments). (**G**) IB analysis of cytochrome C (CYT C) and TUB protein levels in fractions enriched in mitochondrial (MITO) or cytosolic (CYTO) proteins prepared from H1299 cells expressing

ectopic full-length MDM2 (FL), MTS-MDM2 (MTS), or MDM2 1-291 (1-291). (**H**) IF analysis of Cytochrome C (CytC) localization in H1299 cells expressing MTS-MDM2. Co-localization of MTS-MDM2 (green) and CytC (red) indicates absence of CytC release from mitochondria. Nuclei were stained with DAPI (blue). Scale bar: 10 μm. (**I**) IB analysis of cleaved caspase 3 and TUB (loading control) in H1299 cells expressing full-length MDM2 (FL), MTS-MDM2 (MTS) or control cells transfected with empty vector (Empty). Whole-cell lysates of H1299 cells treated with 1 μM staurosporine for 3 hours were used as a positive control for caspase 3 cleavage.

**$p \leq 0.01$ indicates statistical significance of the observed differences. ns=not significant.

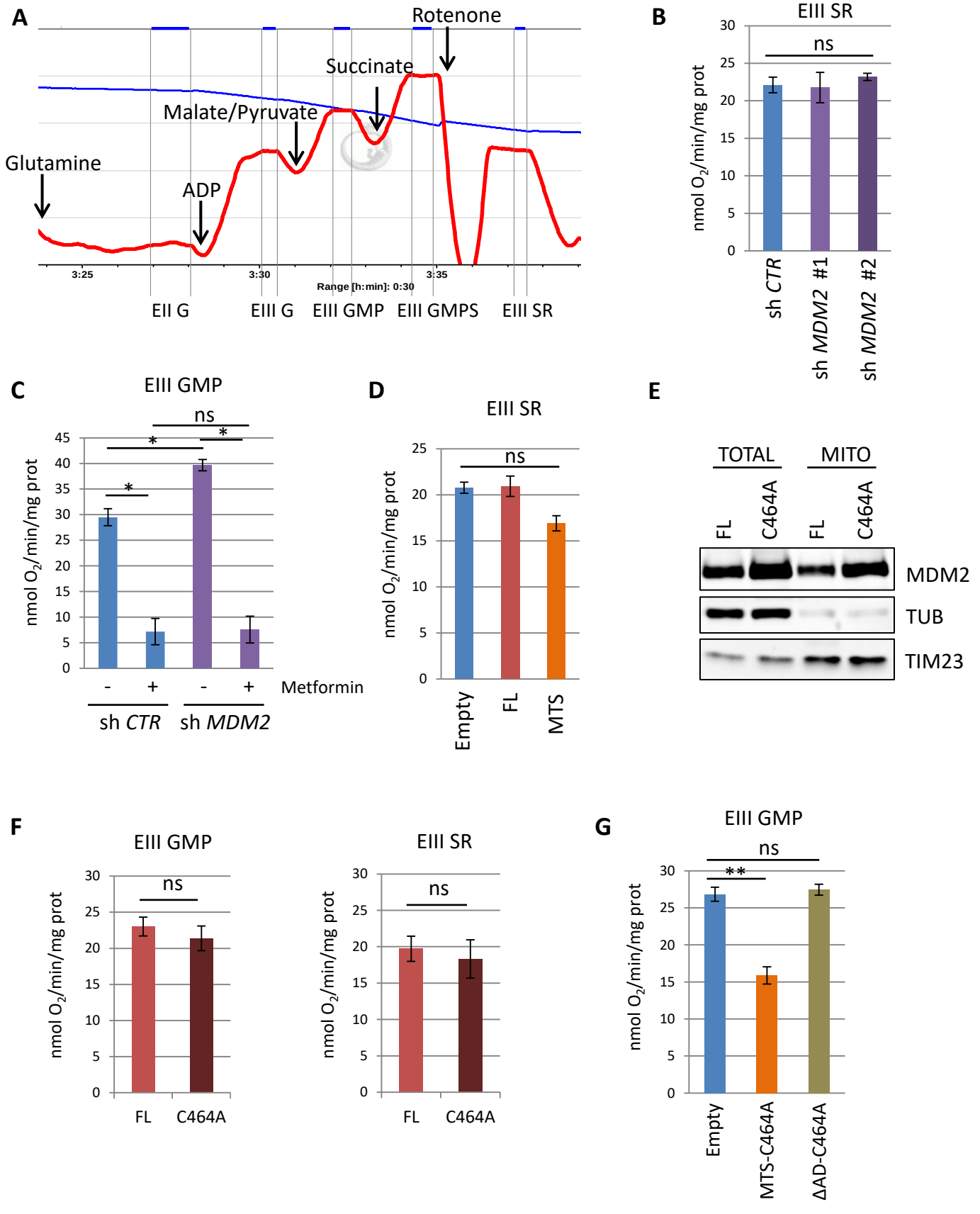
A
Rotenone
Succinate
Malate/Pyruvate
Glutamine
ADP
3:25
3:30
3:35
Range [h:min]: 0:30
EII G
EIII G
EIII GMP
EIII GMPS
EIII SR
B
EIII SR
ns
nmol O2/min/mg prot
sh CTR
sh MDM2 #1
sh MDM2 #2
C
EIII GMP
ns
*
*
*
nmol O2/min/mg prot
-
+
-
+
Metformin
sh CTR
sh MDM2
D
EIII SR
ns
nmol O2/min/mg prot
Empty
FL
MTS
E
TOTAL
MITO
FL
C464A
FL
C464A
MDM2
TUB
TIM23
F
EIII GMP
ns
nmol O2/min/mg prot
FL
C464A
EIII SR
ns
nmol O2/min/mg prot
FL
C464A
G
EIII GMP
ns
**
nmol O2/min/mg prot
Empty
MTS-C464A
ΔAD-C464A

Figure S4, related to Figure 4. (**A**) Schematic representation of the oxygraphy protocol developed to measure oxygen consumption using the Oroboros respirometer. Oxygen concentration (blue) and oxygen flux (red) are expressed as a function of time. Respiration driven by complex I (CI), measured in the presence of glutamine, malate, and pyruvate as substrates (EIII GMP), or by complex II (CII), measured in the presence of the CI inhibitor rotenone and succinate as a substrate (EIII SR) were analyzed. Data recording was started after cell permeabilization with Digitonin. (**B**) Oxygen consumption driven by CII (EIII SR) in H1299 cells expressing control- (sh *Ctr*) or 2 independent *Mdm2*- (sh *Mdm2* #1 and #2) shRNAs (mean ± SEM; n=3). (**C**) CI-driven respiration (EIII GMP) in H1299 cells expressing control- (sh *Ctr*) or Mdm2- (sh *Mdm2*) shRNAs in the presence or the absence of 2 mM Metformin for 24 h (mean ± SEM; n=3). (**D**) CII-driven respiration (EIII SR) in H1299 cells expressing ectopic FL-MDM2 (FL), MTS-MDM2 (MTS) or in control cells transfected with empty vector (Empty) (mean ± SEM; n=3). (**E-G**) MDM2 E3 ligase function is dispensable for its mitochondrial localization and the control of mitochondrial respiration. (**E**) IB analysis of the subcellular localization of FL-MDM2 and of a MDM2 isoform harboring the C464A mutation (C464A) in H1299 cells, using whole-cell lysates (TOTAL) or extracts prepared from purified mitochondria (MITO). (**F**) CI- (EIII GMP) and CII- (EIII SR) driven respiration were determined in H1299 cells transiently transfected with vectors encoding FL-MDM2 or MDM2-C464A (mean ± SEM; n=3). (**G**) CI- (EIII GMP) driven respiration was determined in MDM2-depleted H1299 cells transduced with lentiviruses encoding sh*MDM2*-resistant versions of MTS-MDM2-C464A or ΔAD-MDM2-C464A (mean ± SEM; n=3).

*p ≤ 0.05 and **p ≤ 0.01 indicate statistical significance of the observed differences. ns = not significant.

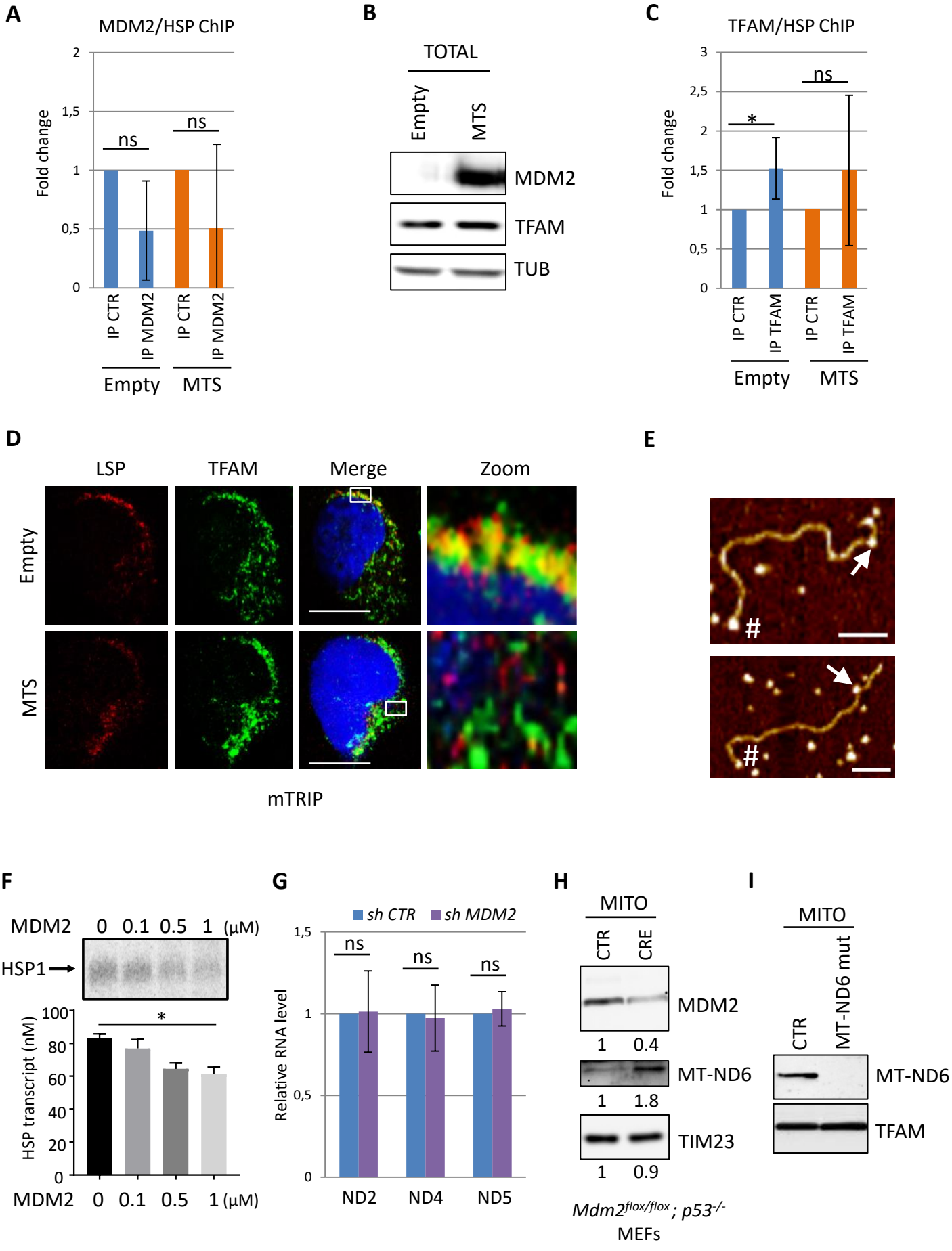
A
MDM2/HSP ChIP
Fold change
2
1,5
1
0,5
0
ns
ns
IP CTR
IP MDM2
IP CTR
IP MDM2
Empty
MTS
B
TOTAL
Empty
MTS
MDM2
TFAM
TUB
C
TFAM/HSP ChIP
Fold change
3
2,5
2
1,5
1
0,5
0
*
ns
IP CTR
IP TFAM
IP CTR
IP TFAM
Empty
MTS
D
LSP
TFAM
Merge
Zoom
Empty
MTS
mTRIP
E
#
#
F
MDM2 0 0.1 0.5 1 (μM)
HSP1
HSP transcript (nM)
100
80
60
40
20
0
*
MDM2 0 0.1 0.5 1 (μM)
G
sh CTR
sh MDM2
Relative RNA level
1,5
1
0,5
0
ns
ns
ns
ND2
ND4
ND5
H
MITO
CTR
CRE
MDM2
1 0.4
MT-ND6
1 1.8
TIM23
1 0.9
Mdm2flox/flox; p53-/-
MEFs
I
MITO
CTR
MT-ND6 mut
MT-ND6
TFAM

Figure S5, related to Figure 5. (**A**) Quantitative chromatin immunoprecipitation (qChIP) experiments evaluating MDM2 recruitment to the mtDNA Heavy Strand Promoter (HSP) in H1299 cells expressing MTS-MDM2 (MTS) or in control cells transfected with the empty vector (Empty). Results are represented as the relative ratio between the mean value of immunoprecipitated chromatin (calculated as a percentage of the input) with a polyclonal MDM2 antibody (N20) and that obtained with a control irrelevant antibody (mean ± SEM; n=3). (**B**) Immunoblot analysis of MDM2, TFAM and TUBULIN (TUB) (loading control) protein levels in whole-cell extracts (TOTAL) prepared from H1299 cells expressing MTS-MDM2 (MTS) or control cells transfected with the empty vector (Empty). (**C**) qCHIP experiments evaluating the recruitment of TFAM to the HSP in the same cells than in (A). (**D**) Confocal microscopy analysis of TFAM (green) recruitment to the LSP (red) following the mTRIP procedure in H1299 cells expressing MTS-MDM2 (MTS) or CTR cells transfected with the empty vector (Empty). Nuclei were stained with Hoechst. Insets represent high-magnification of merged images (Zoom). Scale bars: 1 µM. (**E**) In vitro binding assay using purified recombinant MDM2 and a 1.6 Kb biotinylated DNA probe of the mitochondrial genome encompassing the LSP and the HSP1. 2 representative AFM images showing binding of recombinant MDM2 to the regulatory region of mtDNA (arrow) are shown. # indicates the biotinylated 5' end of the probe used for orientation. Scale bar: 100 nm. (**F**) Upper panel: Autoradiography of a representative in vitro mitochondrial transcription assay using a dual-promoter template performed in the presence of increasing concentrations of recombinant MDM2. Lower panel: Histobars represent the quantification of HSP-driven transcription (mean ± SEM; n=3). (**G**) RT-qPCR analysis of *MT-ND2*, *MT-ND4* and *MT-ND5* RNA levels in H1299 cells expressing control- (sh *Ctr*) or *MDM2*- (sh *MDM2*) shRNAs (mean ± SEM; n=3). (**H**) Quantitative immunoblot analysis of MT-ND6, MDM2 and TIM23 (loading control) protein

levels in extracts prepared from purified mitochondrial isolated from *Mdm2*$^{flox/flox}$; *p53*$^{-/-}$ primary MEFs transduced with control (CTR) or CRE-expressing retroviruses (CRE). (**I**) Immunoblot analysis with anti-MT-ND6 and anti-TFAM antibodies of extracts prepared from purified mitochondria isolated from control (CTR) 3T3 cells or an isogenic cell line harboring a mutation inducing a frame shift in the MT-*ND6* coding sequence (*delC13887*) that abolishes its expression. Equal loading was verified by TFAM protein level. *p ≤ 0.05 indicates statistical significance of the observed differences. ns = not significant.

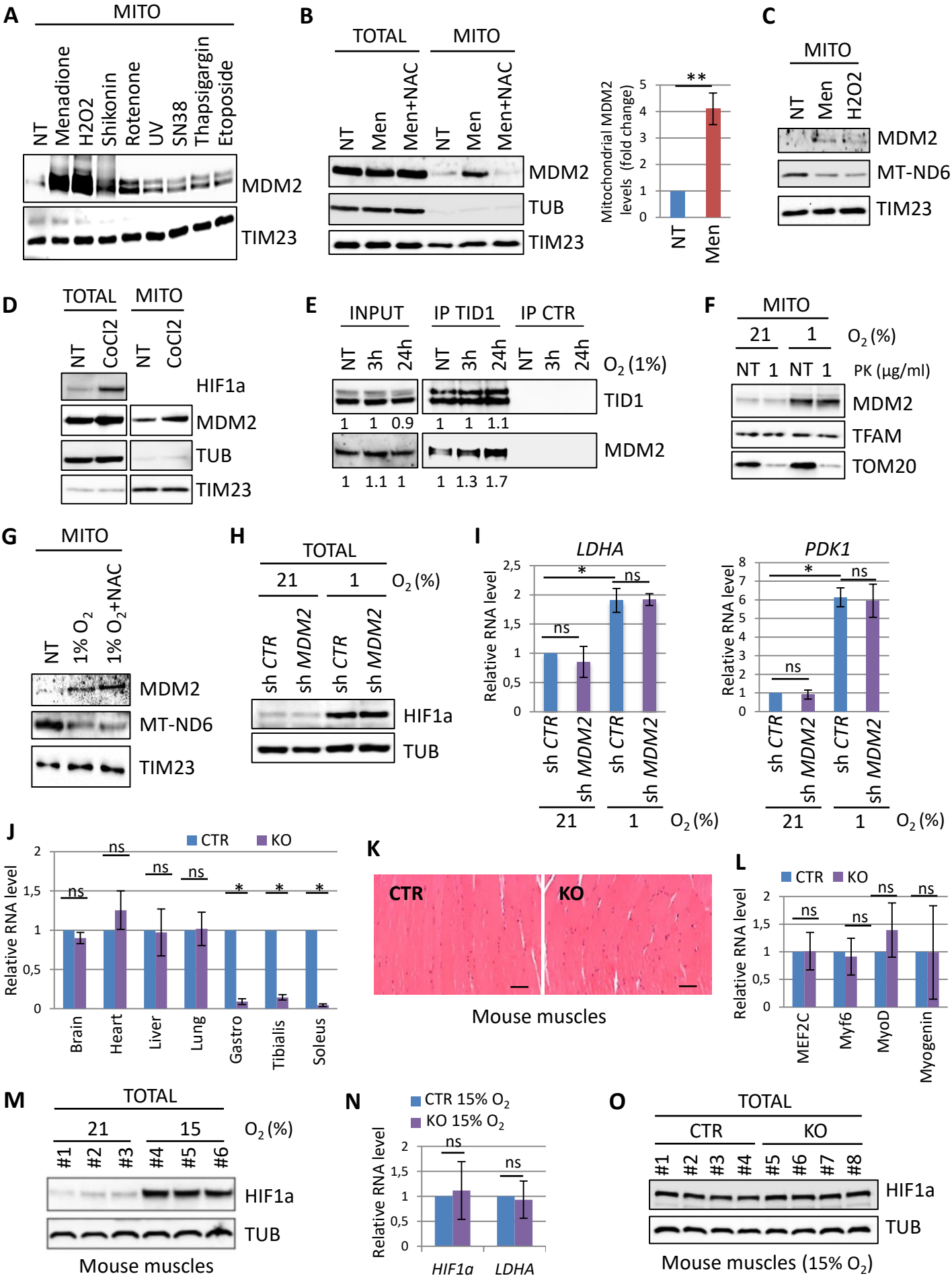
A
MITO
NT
Menadione
H2O2
Shikonin
Rotenone
UV
SN38
Thapsigargin
Etoposide
MDM2
TIM23
B
TOTAL
MITO
NT
Men
Men+NAC
MDM2
TUB
TIM23
Mitochondrial MDM2 levels (fold change)
**
C
MITO
NT
Men
H2O2
MDM2
MT-ND6
TIM23
D
TOTAL
MITO
NT
CoCl2
HIF1a
MDM2
TUB
TIM23
E
INPUT
IP TID1
IP CTR
NT
3h
24h
O2 (1%)
TID1
MDM2
1 1 0.9
1 1 1.1
1 1.1 1
1 1.3 1.7
F
MITO
21
1
O2 (%)
NT 1 NT 1
PK (µg/ml)
MDM2
TFAM
TOM20
G
MITO
NT
1% O2
1% O2+NAC
MDM2
MT-ND6
TIM23
H
TOTAL
21
1
O2 (%)
sh CTR
sh MDM2
HIF1a
TUB
I
LDHA
PDK1
Relative RNA level
*
ns
sh CTR
sh MDM2
21
1
O2 (%)
J
CTR
KO
Relative RNA level
ns
*
Brain
Heart
Liver
Lung
Gastro
Tibialis
Soleus
K
CTR
KO
Mouse muscles
L
CTR
KO
Relative RNA level
ns
MEF2C
Myf6
MyoD
Myogenin
M
TOTAL
21
15
O2 (%)
#1 #2 #3 #4 #5 #6
HIF1a
TUB
Mouse muscles
N
CTR 15% O2
KO 15% O2
Relative RNA level
ns
HIF1a
LDHA
O
TOTAL
CTR
KO
#1 #2 #3 #4 #5 #6 #7 #8
HIF1a
TUB
Mouse muscles (15% O2)

Figure S6, related to Figure 6. (**A**) Immunoblot analysis of mitochondrial MDM2 and TIM23 (loading control) protein levels in H1299 cells expressing ectopic FL-MDM2 and subjected to different stress conditions. (**B**) Immunoblot analysis of endogenous MDM2, TUB and TIM23 protein levels in whole-cell lysates (TOTAL) or extracts prepared from purified mitochondria (MITO) isolated from H1299 cells treated with Menadione (Men) for 1 h in the absence or the presence of the ROS scavenger N-acetyl-cysteine (NAC). Histobars represent the relative level of endogenous mtMDM2 determined by quantitative immunoblotting (mean ± SEM; n=3). (**C**) IB analysis of MDM2, MT-ND6 and TIM23 (loading control) proteins levels in extracts prepared from purified mitochondria (MITO) isolated from H1299 cells treated with Men or H2O2 for 3h. (**D**) IB analysis of HIF1α, MDM2, TUB and TIM23 (loading controls) proteins levels in whole-cell lysates (TOTAL) or extracts prepared from purified mitochondria (MITO) isolated from H1299 cells treated with Cobalt Chloride (CoCl2) for 24h. (**E**) Co-immunoprecipitation assays showing increased association between endogenous MDM2 and TID1 in H1299 cells cultured in 21% or 1% O_2 for 3 or 24 h. (**F**) Protease protection assays on purified mitochondria isolated from H1299 cells cultured in an atmosphere containing 21% or 1% O_2 for 3h. (**G**) IB analysis of endogenous MDM2, MT-ND6 and TIM23 (loading control) protein levels in extracts prepared from purified mitochondria (MITO) isolated from H1299 cells cultured in 21% or 1% O_2 for 3h in the absence or in the presence of the ROS scavenger N-acetyl-cysteine (NAC). (**H**) IB analysis of endogenous HIF1α and TUB (loading control) in whole-cell lysates (TOTAL) prepared from H1299 cells cultured in 21% or 1% O_2 for 3 h. (**I**) RT-qPCR analysis of the HIF1α-target genes *LDH-A* and *PDK1* mRNA levels in H1299 cells expressing control- (sh *Ctr*) or *MDM2*- shRNAs (sh *MDM2*) cultured in 21% O_2 or 1% O_2 for 3h (mean ± SEM; n=3). (**J**) Tissue specificity and efficiency of Cre-mediated recombination of the *Mdm2* flox allele in $Mdm2^{KO(ACTA)}$; $p53^{KO}$ mice and control littermates. RT-qPCR analysis

of *Mdm2* mRNA levels in different organs of 12 to 16 week-old *Mdm2*$^{KO(ACTA)}$; *p53*^{KO} (KO) and *Mdm2*$^{CTR(ACTA)}$; *p53*^{KO} (CTR) males. (**K**) Hematoxylin and eosin (H&E) staining of striated muscle sagittal sections prepared from 12 to 16 week-old *Mdm2*$^{CTR(ACTA)}$*; p53*^{KO} (CTR) and *Mdm2*$^{KO(ACTA)}$*; p53*^{KO} (KO) males. Scale bar: 200 µm. (**L**) RT-qPCR analysis of *MEF2C*, *Myf6*, *MyoD* and *Myogenin* mRNA levels in the hind limb muscles of *Mdm2* CTR and KO males (mean ± SEM; n=6 mice per group). (**M**) IB analysis of HIF1α and TUB (loading control) protein levels in whole-cell lysates (TOTAL) prepared from skeletal muscles of C57Bl/6 mice placed under normoxic (21% O_2) or mild hypoxic (15% O_2) conditions for 3 h. (**N**) RT-qPCR analysis of *HIF1α* and *LDH-A* mRNA levels in the hind limb muscles of *Mdm2* CTR and KO males mice exposed to 15% O_2 for 3 h (mean ± SEM; n=6 mice per group). (**O**) IB analysis of total HIF1α and TUB (loading control) protein levels in the hind limb muscles of *Mdm2* CTR and KO mice exposed to 15% O_2 for 3 h.

*p ≤ 0.05 and **p ≤ 0.01 indicate statistical significance of the observed differences. ns = not significant.

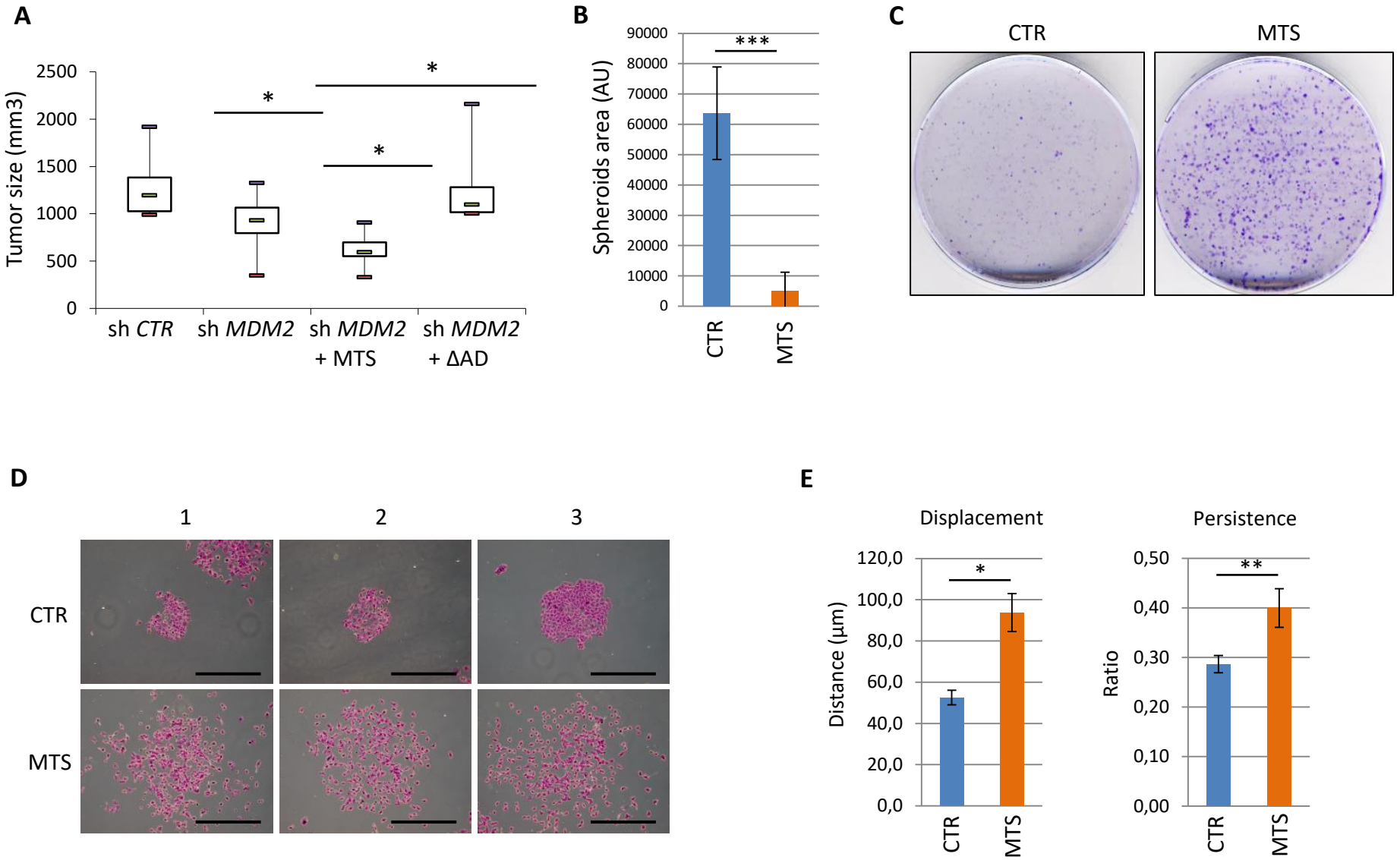
A
Tumor size (mm3)
2500
2000
1500
1000
500
0
*
*
*
sh CTR
sh MDM2
sh MDM2 + MTS
sh MDM2 + ΔAD
B
Spheroids area (AU)
90000
80000
70000
60000
50000
40000
30000
20000
10000
0
***
CTR
MTS
C
CTR
MTS
D
1
2
3
CTR
MTS
E
Displacement
Distance (µm)
120,0
100,0
80,0
60,0
40,0
20,0
0,0
*
CTR
MTS
Persistence
Ratio
0,50
0,40
0,30
0,20
0,10
0,00
**
CTR
MTS

Figure S7, related to Figure 7. (**A**) Nude mice were subcutaneously xenografted with control or MDM2-depleted H1299 cells transduced with lentiviruses encoding shRNA MDM2-resistant versions of MTS-MDM2-C464A or ΔAD-MDM2-C464A. Box and whisker plots represent the tumor volume (mean ± SD, n=10 tumors per group) in each experimental group measured when one animal reached the ethical endpoint. (**B**) Quantification of spheroid size in anchorage-independent growth conditions of MDM2-depleted H1299 cells transduced with a lentivirus encoding MTS-MDM2-C464A (MTS) or with an empty lentivirus (CTR). AU=arbitrary units. (**C**) Clonogenic potential of H1299 cells transduced with a lentivirus encoding MTS-MDM2-C464A (MTS) or with an empty lentivirus (CTR). Monolayer cultures were microphotographed after Crystal violet staining, 8 days after seeding a single-cell suspension. (**D**) Microphotographs of representative clones of the same monolayer cultures as in (C) observed by bright field microscopy. Scale bar, 1 mm. (**E**) Single cell tracking analysis of H1299 cells transduced with a lentivirus encoding MTS-MDM2-C464A (MTS) or with an empty lentivirus, as indicated. Histobars represent displacement (i.e eucledian distance (μm) between the first and last time points, left panel) and persistance (the ratio of displacement over the total distance travelled, right panel) of randomly selected cells (mean ± SEM; n=100 cells from 3 independent experiments).

*$p \leq 0.05$ and **$p \leq 0.01$ indicate statistical significance of the observed differences.

Table S1. Oligonucleotides used in this study, related to STAR Methods

Name	Sequence	Source
Human LSP Fw (ChIP)	GGA GTC GGA GGG GAA AAT AA	MWG
Human LSP Rv (ChIP)	TTT ATC TTT TGG CGG TAT GC	MWG
Human HSP Fw (ChIP)	CCC ATC CTA CCC AGC ACA	MWG
Human HSP Rv (ChIP)	GGT GTC TTT GGG GTT TGG TT	MWG
Human TBP Fw	TGT GCT CAC CCA CCA ACA AT	MWG
Human TBP Rv	TGC TCT GAC TTT AGC ACC TGT T	MWG
Human MT-ND2 Fw	AGC ACC ACG ACC CTA CTA CT	MWG
Human MT-ND2 Rv	CAT TTG GGC AAA AAG CCG GT	MWG
Human MT-ND4 Fw	TTC CCC AAC CTT TTC CTC CG	MWG
Human MT-ND4 Rv	TGG ATA AGT GGC GTT GGC TT	MWG
Human MT-ND5 Fw	TCG CTT CCC CAC CCT TAC TA	MWG
Human MT-ND5 Rv	ATC CTG CGA ATA GGC TTC CG	MWG
Human MT-ND6 Fw	GGT CAG GGG TTG AGG TCT TG	MWG
Human MT-ND6 Rv	ACT CTT TCA CCC ACA GCA CC	MWG
Human LDHA Fw	ATG GCA ACT CTA AAG GAT CAG C	MWG
Human LDHA Rv	CCA ACC CCA ACA ACT GTA ATC T	MWG
Human PDK1 Fw	CTG TGA TAC GGA TCA GAA ACC G	MWG
Human PDK1 Rv	TCC ACC AAA CAA TAA AGA GTC CT	MWG
Human ZEB1 Fw	GCA CCT GAA GAG GAC CAG AG	MWG
Human ZEB1 Rv	TGC ATC TGG TGT TCC ATT TT	MWG
Human ZEB2 Fw	GGG AGA ATT GCT TGA TGG AGC	MWG
Human ZEB2 Rv	TCT CGC CCG AGT GAA GCC TT	MWG
Human EPHA2 Fw	GGA GGG ATC TGG CAA CTT GG	MWG
Human EPHA2 Rv	CTT CCT CCT GCG GTG GAT AA	MWG
Human B2M Fw	GAG TAT GCC TGC CGT GTG AA	MWG
Human B2M Rv	TGC GGC ATC TTC AAA CCT CC	MWG
Mouse HIF1a Fw	GGG TAC AAG AAA CCA CCC AT	MWG
Mouse HIF1a Rv	GAG GCT GTG TCG ACT GAG AA	MWG
Mouse LDHA Fw	TGG CGA CTC CAG TGT GCC TG	MWG
Mouse LDHA Rv	AGG CAC TGT CCA CCA CCT GCT	MWG
Mouse Mef2c Fw	CAA GTA CAC CGA GTA CAA CGA G	MWG
Mouse Mef2c Rv	GTG AGT GCA TAA GAG GAG TCA G	MWG
Mouse Myf6 Fw	GCT GGA TCA GCA AGA GAA GAT G	MWG
Mouse Myf6 Rv	GCA GGT GCG CAG GAA AT	MWG
Mouse MyoD Fw	CGC TCC AAC TGC TCT GAT G	MWG
Mouse MyoD Rv	CGC CGC CTC ACT GTA GTA	MWG
Mouse MyoG Fw	AGT GAA TGC AAC TCC CAC AG	MWG
Mouse MyoG Rv	GAC GTA AGG GAG TGC AGA TTG	MWG
Mouse MT-ND6 Fw	TGG TTG TCT TGG GTT AGC ATT	MWG
Mouse MT-ND6 Rv	CGA TCC ACC AAA CCC TAA AA	MWG
Mouse TBP Fw	ATC AAC ATC TCA GCA ACC CA	MWG
Mouse TBP Rv	TTG AAG CTG CGG TAC AAT TC	MWG